

A Numerical Case Study of East Asian Coastal Cyclogenesis

SHOU-JUN CHEN* AND LORENZO DELL'OSSO

European Centre for Medium Range Weather Forecasts, Shinfield Park, Reading, England

(Manuscript received 30 May 1985, in final form 21 August 1986)

ABSTRACT

The relative importance of latent heat release and surface sensible heat flux in a case of East Asian coastal cyclogenesis were investigated by performing numerical experiments with the ECMWF limited-area model. In the control experiment that included all physical processes, the cyclone developed rapidly in a way similar to that observed. In the experiment without latent heat feedback, only a shallow low appeared when the upper short-wave trough approached the inverted surface trough situated on the coast, but no further development took place. This suggests that the baroclinic forcing was enhanced by the feedback of physical processes.

An increasingly unbalanced subtropical jet streak, an ageostrophic low-level jet and the associated vertical indirect circulation prior to the major development were well simulated in the Control but they were not simulated in the "dry" experiment (without latent heating). The latent heating had a profound impact on the amplifying jet streak circulation and the vertical coupling within the systems, which appeared to prime the rapid cyclogenesis along the coast.

The sensible heating contributed nearly 18% to the surface development. It helped to build a potential temperature contrast along the coast below 900 mb. Without sensible heating, the model latent heat release was reduced. The results from the experiment without sensible and latent heating indicated that, the impact of sensible heating was partly through the moist process rather than direct heating.

1. Introduction

During winter time, the subtropical and polar jet streams merge over the East Asian continent. The confluence of the large-scale upper flows causes the development of a few cyclones which can be observed over Mongolia and Northeast China (Staff members, Academia Sinica, 1958). Over the mainland, many cyclonic circulations appear as shallow lows or inverted troughs. But, if these weak disturbances move off the coast, they can deepen very quickly. A drop of central pressure of more than 20 mb in 24 h, reaching the critical value of a "bomb" as defined by Sanders and Gyakum (1980), is common. The cyclones which develop over the Yellow Sea and East Sea often cause strong gales and the cold air west of the cyclones spread southward as an outbreak of winter monsoon. Furthermore, as the cyclones continue to deepen and move northeastward they eventually become huge lows over the Aleutian region as a part of semipermanent action-center. Thus the behavior of coastal cyclones is important for weather forecasting over East Asia as well as understanding the general circulation.

Among the synoptic and numerical studies of North American coastal cyclones, works on the major coastal cyclone of 18–19 February 1979 (known as the Presidents' Day Cyclone) by Bosart (1981) and Uccellini

et al. (1983, 1984, 1985) are especially noteworthy. They pointed out that the main features and processes contributing to the evolution of that particular cyclone are: 1) significant sensible heat transport over the ocean and latent heat release along the east coast, 2) coastal frontogenesis, 3) a polar jet streak propagating eastward, an amplifying subtropical jet (STJ) streak located over the eastern United States and an intense low level jet (LLJ) located along the east coast prior the development. Case studies of East Asian coastal cyclones are rare. An early synoptic study showed that a wide precipitation area occurred over the coast before the cyclone was initiated (Chen, 1954), suggesting that the impact of the latent heat release may be a factor that helps further development. Hoskins (1980) presented a numerical case study of cyclone development over Western Pacific, Chen et al. (1983) performed some numerical experiments for an AMTEX '75 oceanic cyclone which started over the ocean south of Japan and developed into an intense extratropical cyclone during the next 24 hours. Both the authors found that latent heating had a profound impact on the intensity of the storm. But those experiments only concern oceanic cyclones. Thus, the mechanism of the explosive development of the cyclone off the East Asian coast is still not yet clear.

The aim of this paper is to examine the impact of latent and sensible heating on the development of East Asian coastal cyclone through numerical experiments. The model used for the experiments is the limited area

* On leave from Department of Geophysics, Peking University, Beijing, China.

version of the ECMWF global grid point model (Burrige and Hasler, 1977). It uses σ as vertical coordinate with 15 levels and a horizontal resolution of 1.875° of latitude and longitude. The physics of the model contains large scale latent heating, a modified Kuo's convective parameterization scheme (Kuo, 1974), planetary boundary physics, radiation and the surface fluxes of sensible and latent heat. A more detailed description of the model physics can be found in Tiedtke et al. (1979).

Four simulations were performed: 1) The control experiment, referred to as CON, includes all the model physics. 2) This experiment is similar to the CON but the latent heat is excluded in the model; it is referred to as NLH. 3) In this experiment the surface sensible heat flux is excluded; it is referred to as NSH. 4) In this fourth experiment both sensible and latent heating

are excluded; it is referred to as NSLH. Each simulation started at 0000 UTC 28 November 1982, and the model was integrated for a 48 h period. The initial 500 and 1000 mb maps are shown in Fig. 1a, b. The model domain was 15°N – 65°N , 70°E – 180°E , and the boundary values were obtained from analyses every 12 hours and linearly interpolated for every time step.

2. Synoptic event and control experiment

At 0000 UTC 28 November 1982, cyclogenesis occurred along the East Asian coast and the initial shallow inverted trough developed into a major cyclone within two days. Figure 1 shows the 1000 and 500 mb analyses for 0000 UTC 28 November and 0000 UTC 30 November 1982. At 0000 UTC 28, an anticyclonic circulation at 1000 mb occupied the southern part of the

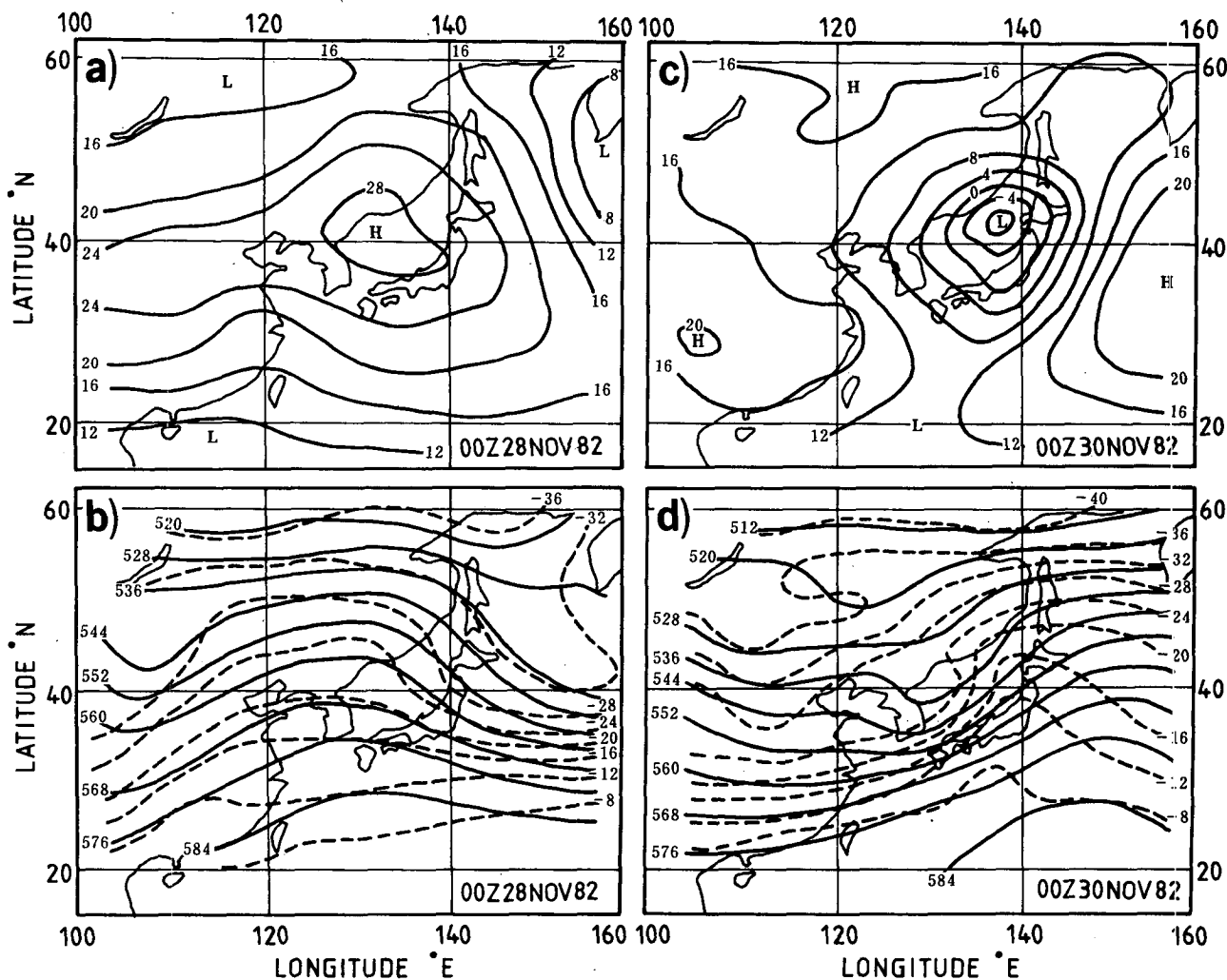


FIG. 1. ECMWF analyses for 0000 UTC 28 November 1982, (a) 1000 mb and (b) 500 mb. (c) and (d) same as in (a) and (b), but for 0000 UTC 30 November 1982. Geopotential height contours (solid lines) every 40 gpm, temperature contours (dashed lines) every 4°C .

mainland with cold air established over eastern China. The inverted trough was located to the west of the coast and oriented approximately north-south along 120°E . At 500 mb, the dominant feature over China was a short-wave trough along 108°E which extended from Gansu to Sichun province. The lag of the thermal trough behind the pressure trough indicates cold advection along the trough line. As the upper trough approached the surface inverted trough, a cyclone started to form at the tip of the surface trough. Bosart (1981) and Uccellini et al. (1984), in their investigation of the President's Day Cyclone, also pointed out that the rapid cyclone spinup was accompanied with the approach of a midtropospheric short-wave trough.

By 0000 UTC 29, a weak cyclonic closed center, with central pressure of 1008 mb formed over Yellow Sea (36°N , 123°E . Figure not shown). The associated fronts became well defined and formed a warm sector. The upper trough slightly deepened and a warm ridge ahead of the trough developed along the coast. Due to the formation of the thermal ridge, the thermal advection increased. This warm ridge is a synoptic feature associated with the coast development (Chen, 1954). The surface low moved northeastward, deepened markedly, and reached a mature stage. In the middle troposphere, the thermal ridge developed further, and the warm advection over the surface warm front became more pronounced. By 0000 UTC 30, the cyclone moved over the Japanese Sea and became a major feature. The central pressure dropped 21 mb within 24 h. From Table 1 it can be seen that the explosive development took place between 0000 UTC 29 and 0000 UTC 30. The upper trough then deepened with further enhancement of the frontal zone and the thermal ridge. As shown later the kinetic energy increased in the wave domain during this period suggesting that the development was due to the internal diabatic processes rather than only to the adiabatic processes.

Uccellini et al. (1984) emphasize the role of the upper STJ and LLJ prior to the development of the President's Day Cyclone. The ageostrophic wind in the entrance region of an anticyclonically curved STJ streak could induce a transverse indirect vertical circulation and strengthen the LLJ. The LLJ would then advect moisture and heat northward contributing to the development. Similar features can be found in this case.

TABLE 1. The observed and simulated central pressure of the cyclone (from 0000 UTC 28 November 1982) every 12 hour (in mb) in CON, NLH, NSH and NSLH experiments, "T" means trough.

	00 h	12 h	24 h	36 h	48 h
Observed	1022(T)	1012	1008	997	987
CON	1022(T)	1015(T)	1007	998	989
NLH	1022(T)	1020(T)	1018(T)	1011	1008
NSH	1022(T)	1017(T)	1010	1002	995
NSLH	1022(T)	1020(T)	1019(T)	1013(T)	1011

Figure 2 depicts the 200 and 850 mb wind and height fields at 0000 UTC 28 and 0000 UTC 29, respectively, the period before the rapid development took place. At 200 mb, as the STJ propagated towards the east coast, it was enhanced both in amplitude and strength. The amplitude increased nearly 5° of latitude and the maximum speed increased 37 m s^{-1} within 24 hours (from 45 m s^{-1} at 0000 UTC 28 to 82 m s^{-1} at 0000 UTC 29). A STJ streak was created over northeast China (45°N , 125°E) near the crest of the ridge by 0000 UTC 29. Thus the flow became highly unbalanced in that the cross-contour flow increased dramatically. The wind was nearly parallel to the height contours, i.e., the STJ was quasi-geostrophic on 0000 UTC 28, while the cross height contour wind became evident on 0000 UTC 29. The ageostrophic wind, greater than 20 m s^{-1} , was directed toward the lower height at nearly a 30° angle along the jet axis. An upper divergence pattern was produced over the initiated surface cyclone area. At 850 mb, the speed of the southerly LLJ along the coast also increased from 10 to 25 m s^{-1} . The trough along the coast was deepened up to 140 gpm from 0000 UTC 28 to 0000 UTC 29. An estimate of the isalobaric wind component was along 10 m s^{-1} , so the intensification of the LLJ may be partly due to the increased isalobaric wind component (Uccellini and Johnson, 1979).

Figure 3a, b depict the results of the CON simulation. It can be seen that the CON simulates the development successfully. The 24-hour forecast predicts the initial cyclogenesis off the coast (Table 1). In the 24-48 h forecasts, the model simulates the explosive development with 19 mb drop of central pressure. In fact, the forecast central pressure is nearly the same as the observed.

Another notable feature of the CON is the correct prediction of the enhancement of the thermal ridge and the front in the middle troposphere. The temperature gradient along the front zone increases to $2^{\circ}\text{C}/100\text{ km}$. The front on the east of the trough increases its intensity and the warm front is pronounced. The simulated trough is as deep as that observed and the trough line tilted northeast-southwest similarly to the observation.

The CON also gives a good simulation of the STJ and LLJ prior to the major development (Fig. 4a, b). The 24 h simulated STJ is amplified and the location of the jet streak is at the right position. The maximum wind speed reaches 67 m s^{-1} , though it is still 15 m s^{-1} lower than that in the analysis the increase is remarkable. The enhanced ageostrophic wind in the jet entrance region is evident and with features similar to the analysis, i.e., it is directed toward lower height along the jet axis. The southerly LLJ is also strengthened with a maximum speed 30 m s^{-1} over south Korea.

Since the major development took place off the coast, detailed observations of the precipitation were not

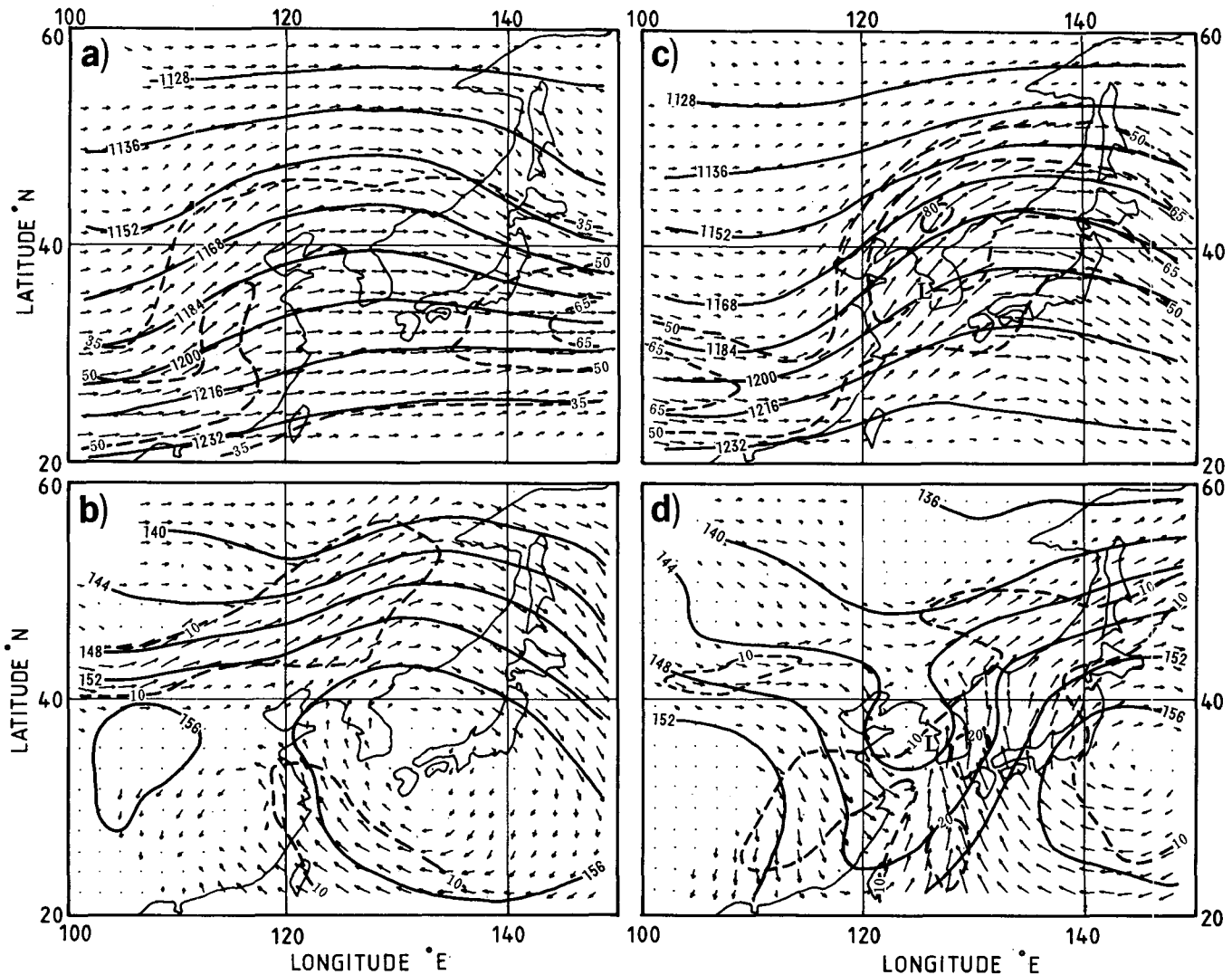


FIG. 2. (a) 200 mb and (b) 850 mb analysed wind and height fields for 0000 UTC 28 November 1982, (c) and (d) same as in (a) and (b), but for 0000 UTC 29 November 1982. Solid lines are height contours in 10 gpm, dashed lines are isotach in m s^{-1} arrows are proportional to the wind speed, "L" denotes the location of the surface cyclonic circulation center.

available for a quantitative comparison, it can only be verified by the satellite imageries. Figure 5a shows the nephanalysis for 1200 UTC 29 November from the Monthly Report of the Meteorological Satellite Centre, JMA (1982). A strong convective belt (X-Y) extended from south Japan to east Taiwan. Another convective center P was located over the Japanese Sea. The 24–48 h accumulated precipitation predicted by CON (Fig. 5b) is qualitatively consistent with the major cloud body.

In view of the discussion above, the CON simulation successfully reproduces the major features of the coastal cyclone; thus, we can assume that the processes involved in the cyclone's developments can be investigated with this numerical model.

3. Numerical results of the no latent heat release experiment

In the NLH experiment, the moist process is included in the model, but the release of latent heat both in large scale nonconvective and convective form is not fed back into the thermal equation.

Figures 3c and 3d show the 1000 and 500 mb maps from the 48 h NLH simulation. The differences between simulation and analysis are remarkable. First, although some development is visible at 1000 mb, the major cyclone is not well predicted. Its intensity is, in fact, much weaker than that in the analysis. The cyclone center does not appear until after 48 h of integration and its central pressure is 1008 mb compared

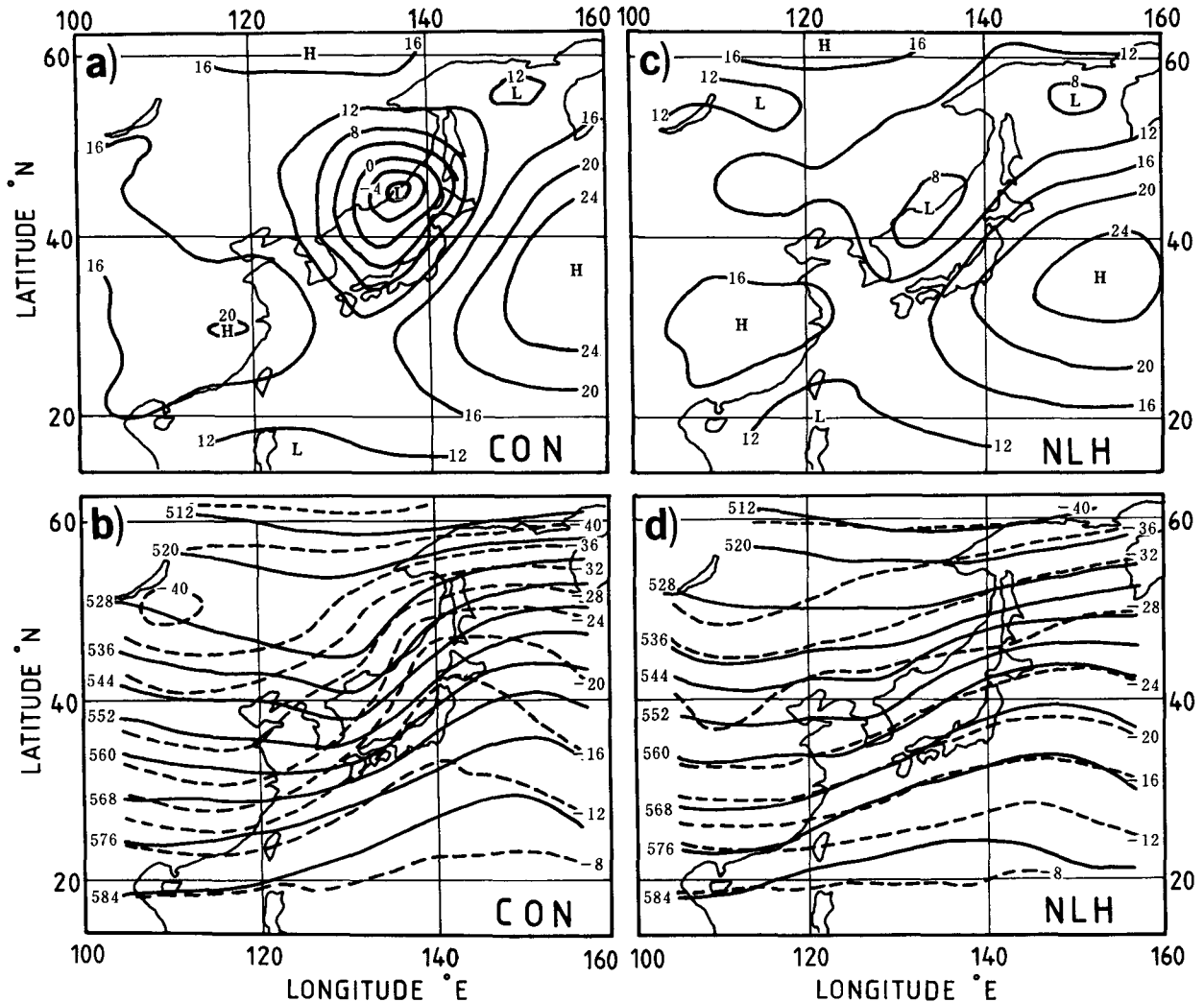


FIG. 3. 48 h simulated (a) 1000 mb and (b) 500 mb maps by CON experiment initialized at 0000 UTC 28 November 1982. (c) and (d) same as in (a) and (b) but by NLH experiment. Isolines as in Fig. 1.

to the analyzed value of 987 and 989 mb in CON. The forcing by the approaching upper trough starts the cyclogenesis but it is incapable of causing the cyclone to deepen rapidly. From Table 1, the differences of central pressure between the NLH and CON every 12 h are: 5, 11, 13 and 19 mb, which shows the accumulated effect of the latent heating.

Another apparent weakness in NLH is the model's inability to forecast the thermal ridge which developed ahead of the trough in conjunction with the enhancement of the front. The horizontal temperature gradient along the strong westerlies at 500 mb becomes weaker as the integration progressed. Initially, the gradient is about 1.7°C/100 km but it decreases to 1°C/100 km after 48 h. The isotherms are nearly parallel to the height contours. The conditions are more nearly

equivalent barotropic and this reduced the baroclinic development.

The enhancement of the thermal ridge and the front due to the latent heating can be illustrated by the difference of simulated 500 mb temperature between CON and NLH (Fig. 6). The maximum difference with temperature up to 8°C occurs over northern Japan, the ridge area. The warming area not consistent with the rainfall area, which is much smaller, shows the nonlinear response of the atmosphere to the latent heat feedback. In other words, the effects of the latent heating are rapidly advected out of the precipitation region. The east coastal cyclone must be considered as a scale interaction problem. The increasing of the east-west temperature contrast between trough and ridge, with a cooling area of less than -4°C located near the

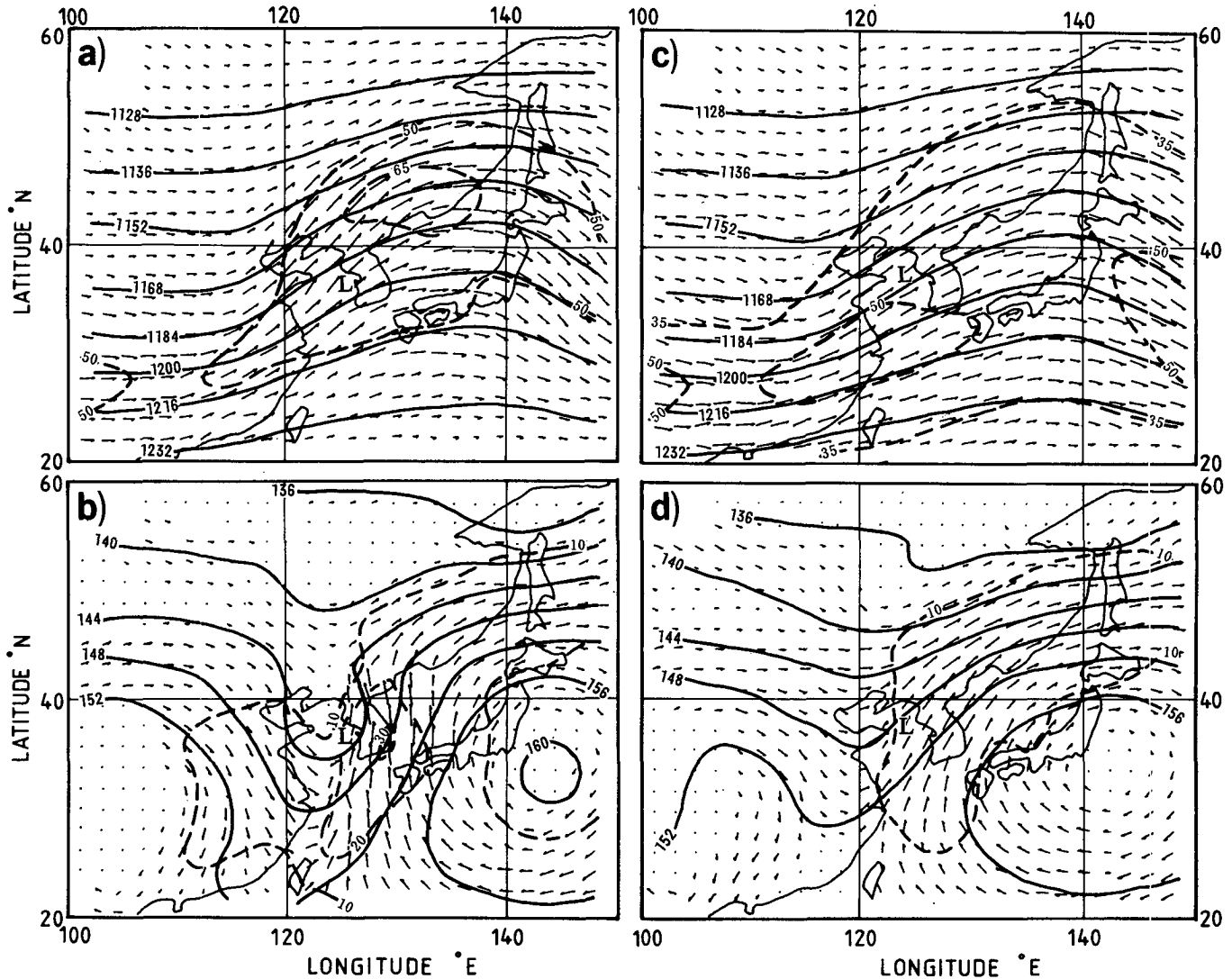


FIG. 4. 28 h simulated (a) 200 mb and (b) 850 mb wind and height fields by CON experiment. (c) and (d) same as in (a) and (b) but for the NLH experiment. Isolines as in Fig. 2.

trough, indicates that the baroclinic instability is also enhanced in the CON.

Finally, the NLH does not simulate the favorable environment prior to the major development (Figs. 4c and 4d). The amplitude of the STJ is damped as it propagates eastward. No jet streak is formed over northeast China. Instead, the jet streak shifts to the lower Yangtze valley (30°N , 120°E), 1000 km southwest to that in the analysis and CON. The flow is nearly parallel to the height contours. The significant ageostrophic wind component along the STJ as in the analysis and CON is absent. At 850 mb, the intensity of LLJ is only 15 m s^{-1} compared with 30 m s^{-1} in the CON. Also, the ageostrophic wind is highly damped. Therefore, it can be inferred that the latent heat release

along the east coast is the main diabatic process which amplifies the jet streaks and the associated phenomena in this case.

The vertical coupling between strengthened STJ and LLJ, strengthened by latent heating, can be found from the simulated vertical velocity fields (Fig. 7). In CON, the rising motion along the east coast, with large value up to $8 \times 10^{-3}\text{ mb s}^{-1}$, is concentrated into a narrow belt (500 km wide) showing the mesoscale α nature of the phenomenon. It is located at the south side of an amplified STJ and on the north side of the LLJ. On the other hand, in NLH, the magnitude of vertical velocity is about 10^{-3} mb s^{-1} , typical value of the synoptic disturbance, and no strong coupling area can be found between STJ and LLJ.

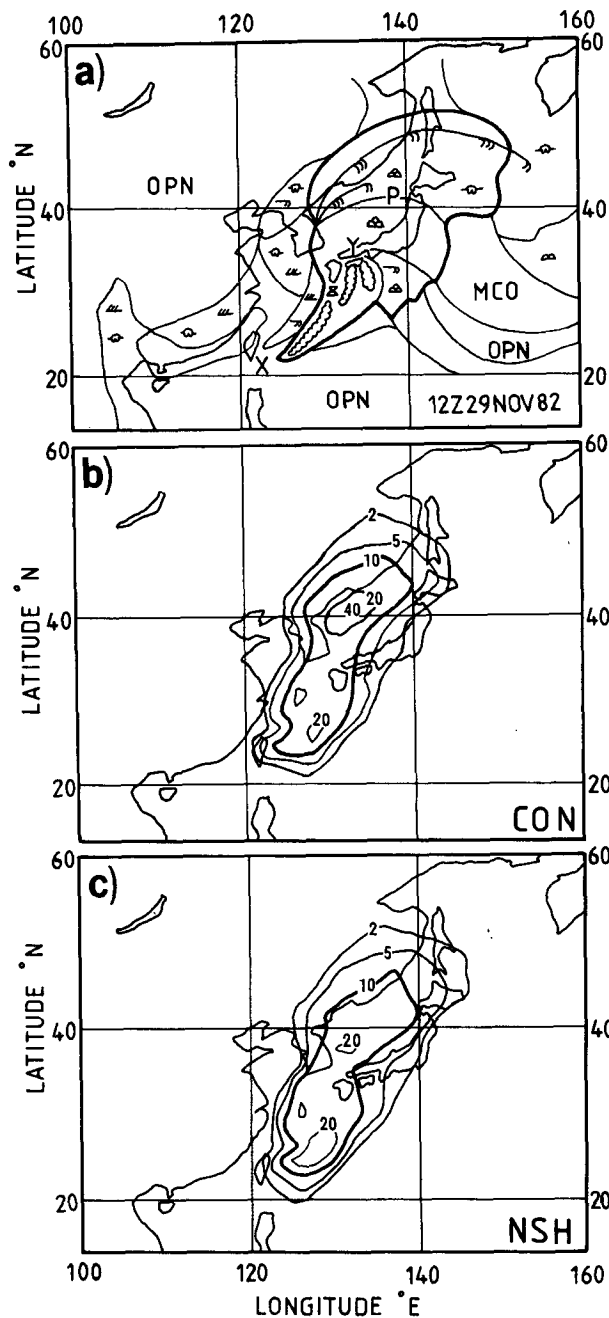


FIG. 5. The nephanalysis for 1200 UTC 29 November 1982, from the Monthly Report of Meteorological Satellite Centre, Japan. Thick line marks the boundary of major cloud system, indicated by X, Y, P. Scalloped lines denote active convective areas, OPN are open areas and MCO is most cloud overcast area. (b) simulated 24-48 h accumulated precipitation for the CON experiment, unit in mm. (c) same as in (a) but for the NSH experiment.

Figure 8 depicts the vertical circulation (along line AB of Fig. 10a), for the 36 h simulation, obtained by subtracting that of NLH from that of CON. The upper-

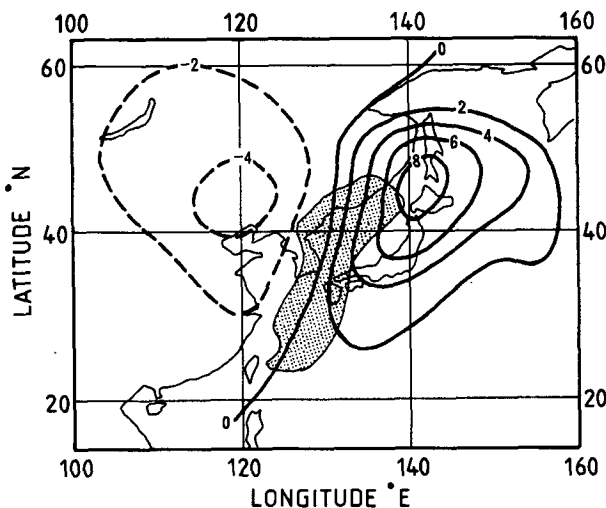


FIG. 6. The difference of 48 h simulated 500 mb temperature for the CON minus NLH experiment, unit in $^{\circ}\text{C}$. The stippled areas denote predicted 24-48 h precipitation greater than 10 mm.

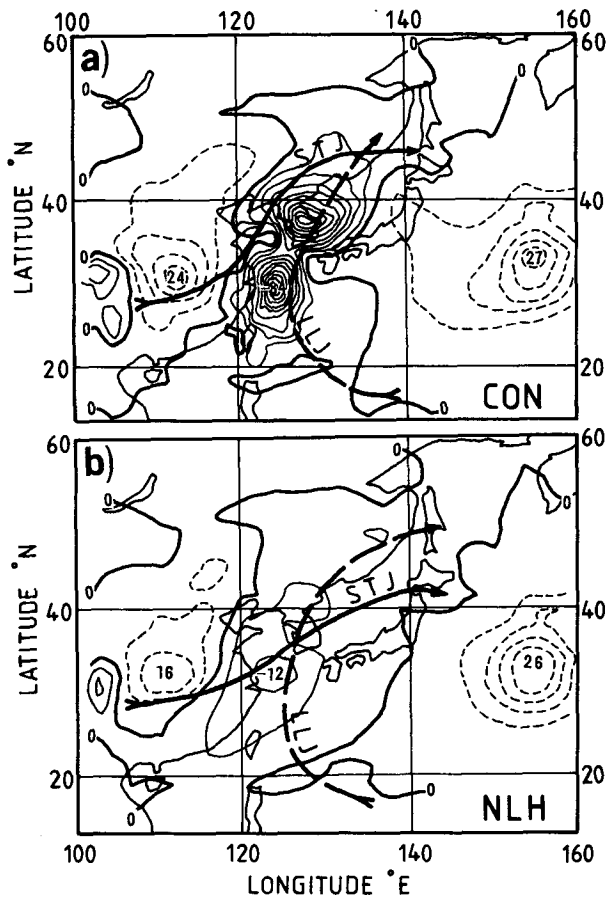


FIG. 7. 24 h simulated vertical velocity (thin lines) at 500 mb for (a) CON and (b) NLH experiments. Isolines is every $5 \times 10^{-4} \text{ s}^{-1}$. Thick arrows indicate STJ and dashed arrows indicate LLJ.

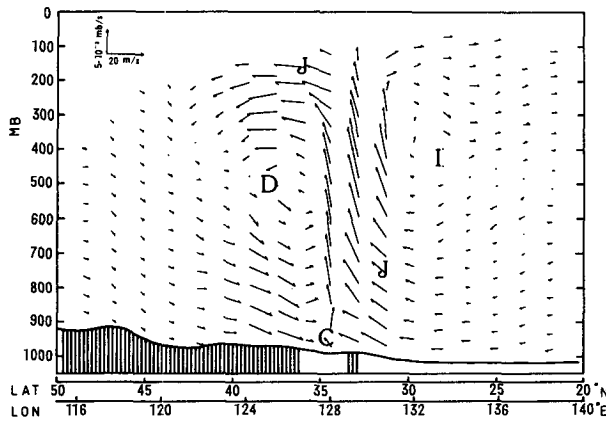


FIG. 8. The difference of 36 h simulated vertical transverse circulation for CON minus NLH experiment, on the cross section from 50°N, 115°E to 20°N, 140°E. Arrows are proportional to the speed (upper left corner). "J" indicate STJ or LLJ, "C" indicates the place where the surface cyclone developed, "I" ("D") indicates the indirect (direct) vertical circulation.

level ageostrophic component is directed to the left of the STJ near the jet axis and to the right, south of jet axis, which is associated with upper-level divergence near and south of the STJ axis, while rising motion beneath the STJ and descent further to the south of the jet completes an indirect circulation (colder air rising and warmer air descending). North of the STJ, a large descending motion occurred. A direct circulation with ascending warmer air and descending colder air was formed on the cyclonic side of the STJ. Its intensity was greater than that of the indirect circulation. The development of the surface cyclone takes place underneath the area of maximum rising motion. The features are similar to that described by Uccellini et al. (1983, 1984). Keyser and Johnson (1984) in a diagnostic case study established that latent heating in the mesoscale convective complex intensified the direct mass circulation in the jet streak entrance region through the forcing of diabatic components of ageostrophic motion. Chen and Dell'Osso (1984) also found such strengthened indirect and direct vertical circulations for a heavy precipitation case over the Asian mainland during summer.

The role of latent heat induced ageostrophic wind in the development can also be confirmed by a diagnostic analysis of the kinetic energy budget in the

model. The calculation is based on the kinetic energy budget equation in σ coordinates presented by Savijarvi (1983):

$$\frac{\partial}{\partial t}(p_s k) = -\nabla \sigma(p_s k \bar{V}) - \frac{\partial}{\partial \sigma}(p_s k \dot{\sigma}) - p_s \bar{V} \times (\nabla \sigma \phi + RT \nabla \sigma \ln p_s) + p_s R k. \quad (1)$$

Here, p_s is the surface pressure, T and ϕ are temperature and geopotential height of the σ surface, $k = \frac{1}{2}(u^2 + v^2)$, the kinetic energy. The term on the left-hand side is the local change and terms on the right-hand side are horizontal kinetic energy flux convergence, vertical kinetic energy flux convergence, kinetic energy generation and the residue respectively. Physically, the residue is the kinetic energy dissipation through surface and internal friction.

The calculation was carried out on the σ surface for the 24–48 h simulation. The area covered from 25° to 55°N and 115° to 150°E, where the development took place.

Table 2 shows the vertically integrated area averaged kinetic energy budget for the NLH and CON. In NLH the local kinetic energy loss is evident, while in the CON the local kinetic energy increase represents the development over a large part of troposphere. The ageostrophic cross height contours flow is the only source of kinetic energy through 24 h period in either run. But in the CON the kinetic energy generation is nearly 2.5 times as large as that in the NLH, which is consistent with the enhancement of the direct circulation in Fig. 8. The increasing of the net gain of the kinetic energy (sum of generation and dissipation) in the CON is 12.6 W m^{-2} while it is 5.7 W m^{-2} in the NLH.

The kinetic energy flux convergence appeared slightly decreased in NLH, but such difference seems insignificant in the total kinetic energy budget, where the development is mainly due to the internal processes.

4. The impact of surface sensible heat flux

In the ECMWF limited-area model, the sea surface temperature is kept constant during the forecast, and the sea surface humidity is equal to the saturation value at the given sea surface temperature. Therefore, excluding the surface sensible heat flux would not alter the sea surface evaporation. Over land, the surface temperature is calculated from a heat balance equation

TABLE 2. Area averaged, vertical integrated kinetic energy budget in the NLH and CON simulations for 24–28 h. Units in W m^{-2} .

	$\frac{1}{g} \int_0^1 \frac{\partial [p_s k]}{\partial t} d\sigma$	$-\frac{1}{g} \int_0^1 [\nabla \sigma (p_s k \bar{V})] d\sigma$	$-\frac{1}{g} \int_0^1 [p_s \bar{V} \cdot (\nabla \sigma \phi + RT \nabla \sigma \ln p_s)] d\sigma$	$p_s R k$
CON	3.1	-9.5	19.7	-7.1
NLH	-2.4	-8.1	7.8	-2.1

which includes processes such as radiation, evaporation and the heat conduction in the soil. If the surface sensible heat flux is excluded in the equation, the land evaporation would be altered. The land evaporation is mainly determined by the water contained in the soil (the surface wetness) which depends on the precipitation. In our case, the main precipitation area is over the sea, thus the land evaporation will not be altered very much by excluding the surface sensible heating in the model (experiment NSH). Actually, the change of land evaporation in NSH is only about 20% of that in the CON.

In NSH, the cyclone develops, Fig. 9, and its size is not very different from that in the CON, e.g., the area enclosed by 0 gpm contour is as large as that in the CON, and the central pressure 6 mb higher. The pressure drop in 48 h, 27 mb in the NSH and 33 mb in

the CON (Table 1), shows that about 18% of the surface development is contributed by the sensible heat. The simulated 500 mb pattern is similar to that in the CON, except that the warm ridge is weaker, the geopotential height is about 40 gpm lower at the crest, and the temperature increases nearly 2°C.

Figure 10a shows the 48 h mean surface sensible heat flux in CON, with a maximum heating of 150 W m⁻² over the Kuroshio area, and another less large value, 50 W m⁻², over the East Sea (30°N, 125°E). The vertical cross section of the 36 h simulated potential temperature difference between CON and NSH (CON - NSH) oriented from land to sea, Fig. 10b, shows that, over the Western Pacific, the potential temperature increases nearly 6°C in CON below 900 mb and 2°C over land. Thus, the surface sensible heating builds a potential temperature gradient of nearly

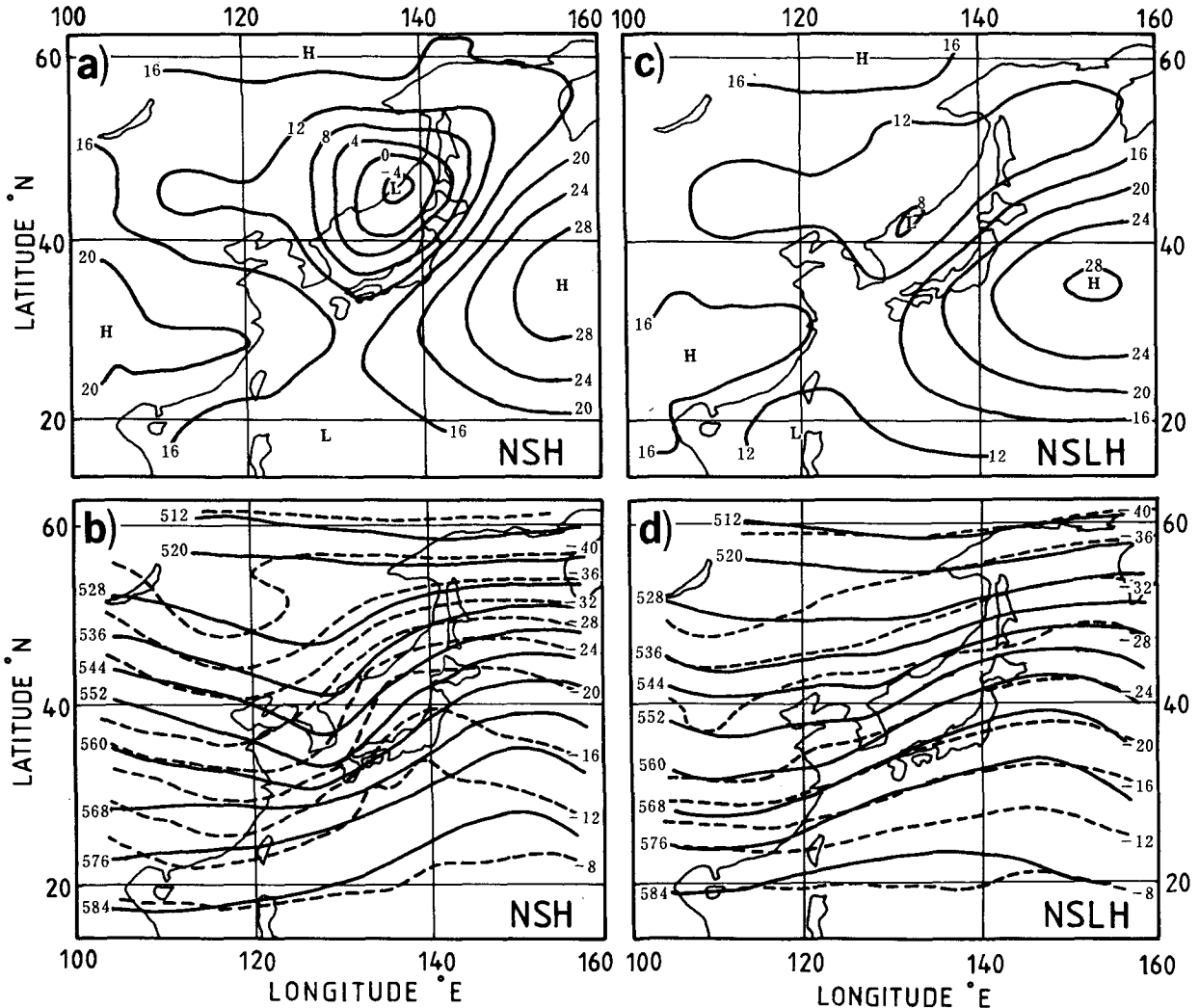


FIG. 9. 48 h simulated (a) 1000 mb and (b) 500 mb maps for NSH experiment. (c) and (d) same as in (a) and (b) but for the NSLH experiment. Isolines are as in Fig. 1.

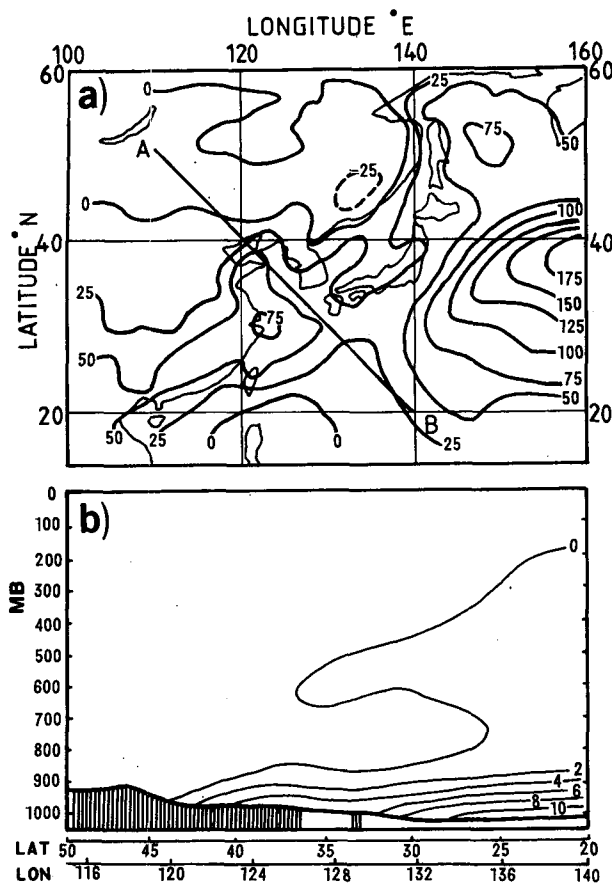


FIG. 10. (a) The simulated 48 h mean surface sensible heat flux in the CON experiment, unit in $W m^{-2}$. (b) The difference of potential temperature on the cross section along line AB in (a) for the CON minus NSH, unit in $^{\circ}C$.

$1^{\circ}C/100$ km along the coast, contributing to the coastal frontogenesis. However such contribution is restricted below 900 mb, while, above 900 mb, the potential temperature fields of the two experiments is almost identical. Thus the baroclinicity in the whole troposphere does not seem to be very much affected by the surface sensible heat.

Bosart and Lin (1984) in their diagnostic study of the Presidents' Day Cyclone obtained the maximum heating up to $400 W m^{-2}$ off the east American coast. Moreover, they estimated the quasi-geostrophic 1000 mb height tendency due to the sensible heating alone in the 1000–850 mb layer and found maximum height falls ~ 100 m/12 h occurring to the north and east of the incipient cyclone. Thus, they inferred that "the sensible heating helps to condition the precyclogenetic environment by enhancing the lower tropospheric baroclinic zone". Uccellini et al., (1983) have conducted numerical experiments for this particular cyclone. They found that in the simulation with latent heating and no sensible heating, "the LLJ and coastal

development were weak when compared to the simulation including sensible and latent heating together". On the other hand, Guo and Hoke,¹ using the NMC nested-grid limited-area model designed by Phillips (1979), carried out some numerical simulations for the cyclone to assess the impact of sensible heating. The control run with all model physics was capable of predicting the explosive development 24 h ahead, however, in the experiment with no sensible heating over the sea, the cyclone still developed, with no evident difference between the two experiments.

Nevertheless, it is unavoidable that excluding sensible heating in the model will alter other physical parameters, e.g., the latent heat release, in the model. Insufficient latent heat release is evident in NSH, although the cause is not yet clear, it may be related to the decrease of the baroclinicity in the boundary layer along the coast (Fig. 10b). The simulated 24–48 h accumulated precipitation in NSH shows the rainfall area as large as that in the CON, but with a total amount smaller, especially over the Japanese Sea: with a maximum ~ 20 mm against the ~ 40 mm of the CON (Fig. 5b).

In an experiment with both sensible and latent heating excluded (NSLH), Figs. 9c and 9d, the 48 h simulation at 1000 and 500 mb is almost identical to that of NLH, Figs. 2c and 2d, the major differences being the area enclosed by the 80 gpm contour at 1000 mb smaller and the center pressure 3 mb higher in NSLH (Table 1). The effect of the sensible heat through the "dry" process is smaller than that through the "moist" process. In other words, in the model the surface sensible heat flux contributes to the development not only through the direct heating but also through the extra latent heating.

5. Summary

A typical major cyclone development off the East Asia coast is studied by performing numerical simulations. From the numerical results it can be seen that:

1. The rapid cyclone development is well simulated in the experiment with the latent heating included, while the experiment with no latent heat feedback process only forecasted a shallow cyclone. So, the pure dry baroclinic forcing does not entirely account for the explosive development.

2. In this case, the environment prior to the development is similar to that of the Presidents' Day Cyclone pointed out by Uccellini et al., (1984), i.e., the coupling of an increasingly unbalanced STJ and a noticeably ageostrophic LLJ. In the control experiment, the enhancement of the STJ and the associated large ageo-

¹ Guo, X. R., and J. E. Hoke, 1985: Office Note 314, NMC, NWS (NOAA), Maryland.

strophic wind combined with the warm moist advection by LLJ prior to the rapid cyclogenesis are well simulated but they are not simulated in the "dry" experiment (without latent heating). This suggests some kind of feedback which is not diagnosed.

3. The kinetic energy budget diagnostics for the CON and NLH show that the development is due to internal processes rather than to those external. The generation of the kinetic energy is greatly enhanced in the CON by the ageostrophic wind induced by latent heat feedback, which causes a net increasing of the kinetic energy in the wave domain.

4. The sea surface sensible heat flux east of the East Asia coast in the model for this case is smaller than the diagnostic value for the Presidents' Day Cyclone from Bosart and Lin (1984). It increases the horizontal potential temperature gradient along the coast only below 900 mb. The sensible heating, that contributes to nearly 18% of the surface development, shows that it is less essential to the cyclone development than the latent heating.

5. As the sensible heating is excluded in the model, the latent heat release is decreased. So, the sensible heating helps the development partly through the increased latent heating. The small difference between the results from NSLH and NLH means that the direct sensible heating is unimportant in the model's ability to forecast the intensification of the coastal cyclone in this case.

These numerical experiments provide just some quantitative assessment of the effects of latent and sensible heating in the development of a coastal cyclone, further studies are needed to clarify the very complicated diabatic processes involved in this phenomenon.

Acknowledgments. The authors wish to express their gratitude to Professor R. J. Reed for his valuable suggestions and comments, and to two anonymous reviewers for their comments that greatly improved the manuscript.

REFERENCES

- Bosart, L. F., 1981: The Presidents' Day snowstorm of 18–19 February 1979: A subsynoptic-scale event. *Mon. Wea. Rev.*, **109**, 1542–1566.
- , and S. C. Lin, 1984: A diagnostic analysis of the Presidents' Day storm of February 1979. *Mon. Wea. Rev.*, **112**, 2148–2177.
- Burridge, D. M., and J. Haseler, 1977: A model for medium range weather forecasts—Adiabatic formulation. ECMWF Tech. Rep. No. 4, 46 pp, ECMWF, Shinfield Park, Reading, England, U.K.
- Chen, H. Y., 1954: Two case study of the development of the cyclone over East Sea. *Acta Meteor. Sin.*, **25**, 213–231.
- Chen, S.-J., and L. Dell'Osso, 1984: Numerical prediction of the heavy rainfall vortex over eastern Asia monsoon region. *J. Meteor. Soc. Japan*, **62**, 730–747.
- Chen, T.-C., C.-B. Chang and D. J. Perkey, 1983: Numerical study of an AMTEX '75 oceanic cyclone. *Mon. Wea. Rev.*, **111**, 1818–1829.
- Hoskins, B. J., 1980: Effect of diabatic processes on transient mid-latitude waves. ECMWF Workshop on Diagnostics of Diabatic Processes, 23–25 April 1980, 85–99. ECMWF, Shinfield Park, Reading, England, U.K.
- Keyser, D. A., and D. R. Johnson, 1984: Effects of diabatic heating on the ageostrophic circulation of an upper tropospheric jet streak. *Mon. Wea. Rev.*, **112**, 1709–1724.
- Kuo, H. L., 1974: Further studies of the parameterization of the influence of cumulus convection on large scale flow. *J. Atmos. Sci.*, **31**, 1232–1240.
- Monthly Report of Meteorological Satellite Centre, 1982. Meteorological Satellite Centre, Tokyo, Japan.
- Phillips, N. A., 1979: A nested grid model. U.S. Dept. of Commerce, NOAA Tech. Rep. NWS 2, 80 pp.
- Sanders, F., and J. R. Gyakum, 1980: Synoptic-dynamic climatology of the "bomb". *Mon. Wea. Rev.*, **108**, 1589–1606.
- Savijarvi, H., 1983: The atmospheric energy budgets over North America, the North Atlantic and Europe based on ECMWF analyses and forecasts. *Tellus*, **35A**, 39–50.
- Staff Members Academia Sinica, 1958: On the general circulation over Eastern Asia II. *Tellus*, **10**, 58–75.
- Tiedtke, M., J.-F. Geleyn, A. Hollingsworth, and J.-F. Louis, 1979: ECMWF model, parameterisation of subgrid scale processes. ECMWF Tech. Rep. No. 10, 45 pp, ECMWF, Shinfield Park, Reading, England, U.K.
- Uccellini, L. W., and D. R. Johnson, 1979: The coupling of upper- and lower-tropospheric jet streaks and implications for the development of severe convective storms. *Mon. Wea. Rev.*, **107**, 682–703.
- , D. Keyser, K. F. Brill and C. H. Wash, 1985: The Presidents' Day cyclone of 18–19 February 1979: Influence of upstream trough amplification and associated tropopause folding on rapid cyclogenesis. *Mon. Wea. Rev.*, **113**, 962–988.
- , R. A. Petersen, P. J. Kocin, M. J. Kaplan, J. W. Zack, and V. C. Wong, 1983: Mesoscale numerical simulations of the Presidents' Day cyclone: Impact of sensible and latent heating on the pre-cyclogenetic environment. *Sixth Conf. Numerical Weather Prediction*, Amer. Meteor. Soc. 45–52.
- , P. J. Kocin, R. A. Petersen, C. H. Wash, and K. F. Brill, 1984: The Presidents' Day cyclone of 18–19 February 1979: Synoptic overview and analysis of the subtropical jet streak influencing the pre-cyclogenetic period. *Mon. Wea. Rev.*, **112**, 31–55.